In Flight SEU/MCU Sensitivity of Commercial Nanometric SRAMs: Operational Estimations

Laurent Artola, Raoul Velazco, Guillaume Hubert, Sophie Duzellier, Thierry Nuns, Bruno Guerard, Paul Peronnard, Wassim Mansour, Fabrice Pancher, and Francoise Bezerra

***Abstract*—A method and the corresponding platform devoted to operational SEE-rate prediction are presented and illustrated by experimental results. Predicted error-rates are in well agreement with results issued from the activation of an SRAM platform, in 90 nm technology node, on board stratospheric balloons flights. Direct ionization of protons is investigated for a 65 SRAM memory virtually boarded on the balloon flight.**

***Index Terms*—Experimental cross-section measurement, in flight experiment, multiple Cell Upset, operational prediction, single event upset.**

I. Introduction

SECONDARY cosmic rays, such as neutrons and protons, can induce Single Event Effects (SEE) in digital electronics via nuclear or direct reactions with silicon (or other) nuclei [1]–[3]. An approach for predicting SEE rates and the corresponding platform, so called MUSCA SEP^3 (MUlti-SCAles Single Event Phenomena Predictive Platform) were presented in previous work [4]. MUSCA SEP^3 aims at calculating, by Monte Carlo simulations, the SEE cross-section and the Soft Error Rate (SER) for the studied circuit/application in both the ground testing and the operational configuration. This platform, was validated thanks to on-board operational results on memories of the SAC-C space mission [4], [5] and experimental results obtained in long-haul commercial flights [6]. In this paper, the electrical simulations have been performed with a new transport and collection charge model, called ADDICT (Advanced Dynamic Diffusion Collection Transient), presented in previous works [7], [8]. This approach based on transient modeling leads to take into account dynamic mechanisms driving the SEE occurrence while a conventional approach using a collected charge model does not.

In today's avionics, the continuous technology downscaling and the incessant grow of the amount of boarded CMOS devices, lead to increase the probability of soft errors. Thus, the industrial community must take into account the impact of radiation effects on the reliability of electronic devices operating in the atmosphere. In a preliminary study [6], an experimental platform was activated during various commercial flights and allowed the detection of Single Event Upsets (SEUs) and Multiple Cell Upsets (MCUs) emphasizing the sensitivity to MCUs of critical order of integrated circuits operating in the earth's atmosphere. This experimental platform includes a memory array of 250 Mbit built from a commercial 90 nm CMOS Static Random Access Memory (SRAM) from Cypress.

In this work are exploited the results issued from the same experimental platform during stratospheric balloon flights. The aim of this paper is to evaluate in details the sensitivity of the same commercial 90 nm SRAM during stratospheric balloon flights, and the multiple contributors, such as secondary cosmic ray (fast and thermal neutrons and protons). The device description has been extracted by a reverse engineering. The device was tested with a thermal neutron beam at Institute Laue-Langevin (ILL). In order to validate the device and sensitivity model a proton accelerator was used at Kernfysisch Versneller Instituut (KVI). Moreover, additional experimental data from recent works [9] has been compared in order to investigate the sensitivity to high energy neutrons. The prediction platform MUSCA SEP^3/ADDICT must be able to perform operational evaluation of the SEE risk for the SRAM memory 90 nm technology node. The soft-error rate (SER) was calculated for an experiment embedded in the payload of stratospheric balloon flights launched in 2010 at Kiruna (Sweden) and in a commercial long-haul flight, the neutron and proton contributors are investigated.

In the final part, the contribution of the direct ionization of protons on the SER during a stratospheric balloon flight had been investigated for 65 nm technology node.

II. Prediction Methodology and Radiation Ground Testing Validations

A. *MUSCA* SEP^3/ADDICT *Methodology*

Multi-scales modeling and physics based on Monte-Carlo simulations have been developed in several institutions, such as ONERA [4], [5], Vanderbilt University [10], [11] or IBM [12], allowing investigating SEE trends. As shown in Fig. 1,

Manuscript received July 13, 2011; revised August 30, 2011; accepted October 08, 2011. Date of publication November 18, 2011; date of current version December 14, 2011.

L. Artola is with ONERA, The French Aerospace Lab, 31055 Toulouse, France and also with CNES, 31401 Toulouse, France (e-mail: laurent.artola@onera.fr).

R. Velazco, W. Mansour, and F. Pancher are with TIMA Labs, 38031 Grenoble, France (e-mail: raoul.velazco@imag.fr; wassim.mansour@imag.fr; farice.pancher@imag.fr).

G. Hubert, S. Duzellier and T. Nuns are with ONERA, The French Aerospace Lab, 31055 Toulouse, France (e-mail: guillaume.hubert@onera.fr; sophie.duzellier@onera.fr).

B. Guerard is with the Institut Laue-Langevin (I.L.L), 38042 Grenoble, France (e-mail: Guerard@ill.fr).

P. Peronnard is with CERN, Geneva 23, CH-1211 Switzerland (e-mail: Paul.peronnard@cern.ch)

F. Bezerra is with CNES, 31401 Toulouse, France (e-mail: francoise.bezerra@cnes.fr).

Color versions of one or more of the figures in this paper are available online at http://ieeexplore.ieee.org.

Digital Object Identifier 10.1109/TNS.2011.2172220

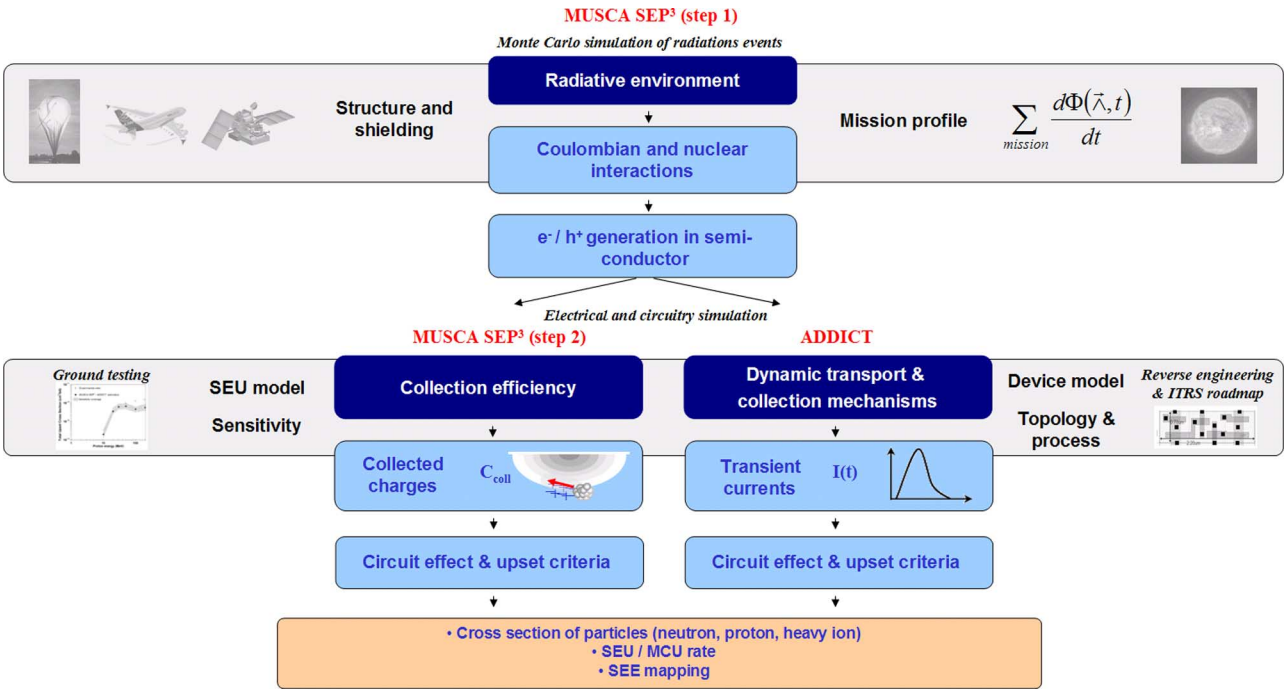

Fig. 1. Schematic principle of the methodology of the MUSCA SEP³/ADDICT prediction platform.

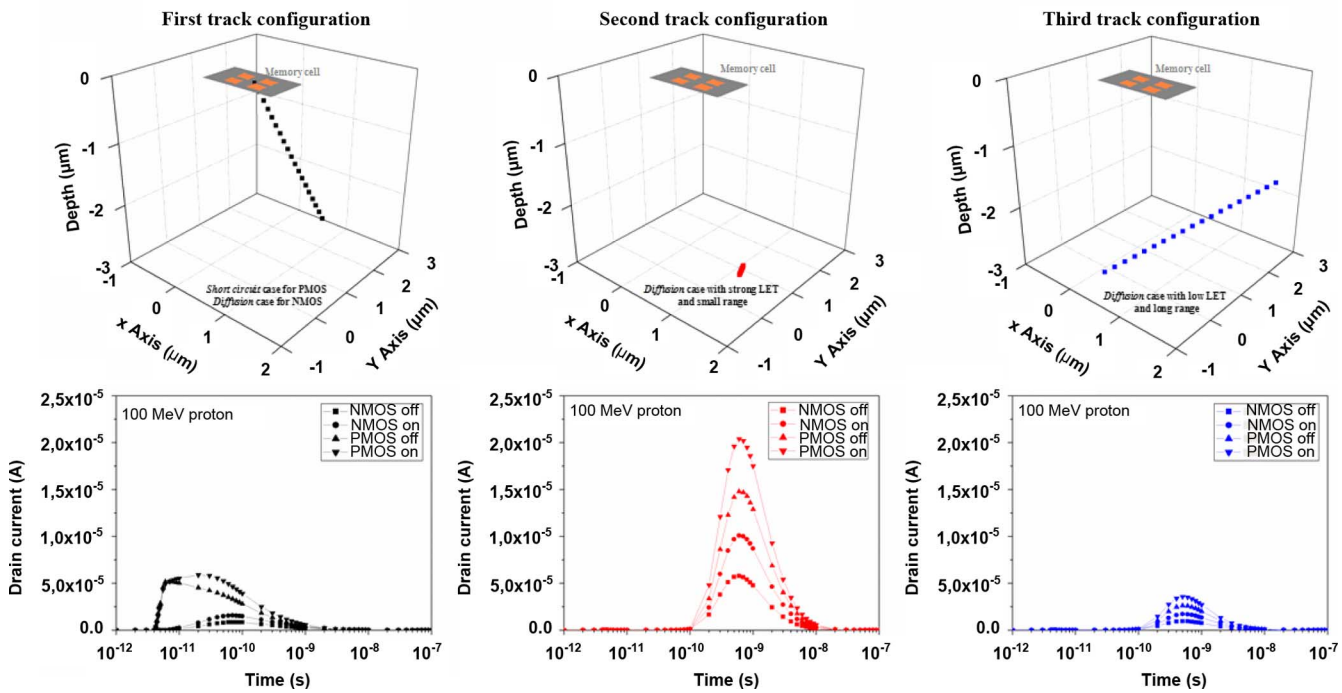

Fig. 2. Representation of the transient responses modeled by ADDICT using the output data (generated charges) of the Monte-Carlo simulation of radiation event (MUSCA SEP³). The presented currents are obtained for three different secondary ion tracks induced by a 100 MeV proton on the 90 nm SRAM memory.

MUSCA SEP³ performs a Monte-Carlo simulation of radiation's events. The outputs (generated charges) are used by ADDICT to simulate the electrical and circuitry response of the device, such as described in [8]. These simulations are based on a transient current modeling taking into account the dynamic transport and collection charges mechanisms. The methodology used in this work allows sequentially modeling all these various physical mechanisms. Fig. 2 emphases the capacity of ADDICT to model different shapes of transient responses whatever the energy and geometric characteristics of the secondary ions induced by a 100 MeV proton on the studied SRAM device. For instance, Fig. 2 shows the transient responses (black curves) in *short circuit* case for the PMOS transistors and *in diffusion* case for the NMOS transistors. The device model contained in the prediction platform is obtained from reverse engineering, and ITRS (International technologic

TABLE I
SUMMARY OF GROUND TESTING PERFORMED TO CORROBORATE AND VALIDATE THE DEVICE AND SENSITIVITY MODEL OF ADDICT

Facility	Location	Beam	Energy range
ILL	Grenoble, France	neutrons	thermal
KVI	Groningen, Netherland	protons	50-184 MeV
ASP & TRIUMF [9]	Aldermaston, UK and Vancouver, Canada	neutrons	14 MeV & 450 MeV

Roadmap for Semiconductor) roadmaps [13]. It describes the topology (drain dimensions and transistor locations) and the process (junction capacitance) of the device [8].

First, the circuit effect and the upset criterion are based on two main parameters which are deduced from information presented in scientific publications. These parameters of the sensitivity model, i.e., the Fan-Out1 (FO-1) and the critical charge, lead to determine the upset occurrence with a unique upset criterion. The transient currents of each inverters of the SRAM cell are used to calculate the maximum charge (Q_{max}) which is compared with the critical charge. If the Q_{max} of one of the inverters is greater than the critical charge, an upset occurs. These calculations are performed with the characteristic time, i.e., the FO-1, as described in details in [8]. Using a large Fan-Out1 results in an overestimation of the maximum collection charge, and consequently in the SEU cross section as well.

After this first step, the sensitivity model is fitted and validated by radiation ground testing.

B. Device Model Definition

The device description used in the electrical and circuitry simulations can be obtained by two approaches: ITRS roadmaps, or if it can be done, by a reverse engineering. The last approach is heavy and expensive but it leads to have a detailed description of the device. In this work, the reverse engineering was performed thanks to the Thales group based at CNES (French Space Agency), in Toulouse. This approach allows obtaining the critical technology parameters for the device model, such as, the topology of the SRAM cell, the dimensions of N and PMOS transistors, and the description of the passivation layers.

In all the cases the sensitivity model used by the predictive platform, needs to be adjusted and validated (critical charge, FO-1). Therefore, radiation ground testing experiments have been performed on various facilities.

C. Preliminary Validations by Radiation Ground Testing

This preliminary step aims at corroborating and validating the device description used in the electrical modeling (ADDICT) of the prediction platform. Radiation ground tests have been performed in 2 different facilities: at ILL, Grenoble (France) for thermal neutrons, at KVI, Groningen (Netherland) for high energy protons.

Besides, additional experimental data of neutron irradiation from ASP and TRIUMF facilities have been used [9]. The whole ground testing is summarized in Table I.

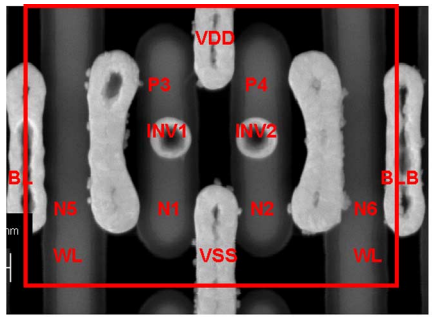

(a)

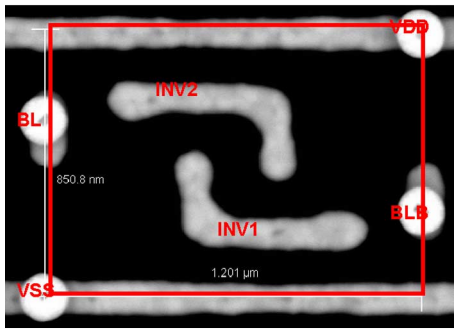

(b)

Fig. 3. Top views of 1.02 μm^2 6T-SRAM cell built by Cypress at poly gate layer (a) and metal 1 (M1) (b).

III. APPLICATION OF THE PREDICTION METHODOLOGY TO A 90 NM SRAM MEMORY

A. Reverse Engineering of 90 nm SRAM

The memory investigated is a high-performance CMOS SRAM, built on bulk silicon, organized as 1 M words of 16 bits. The memory cell is a 6 transistors, high density, 90 nm technology node with dimensions of 1.2×0.85 μm and an area of 1.02 μm^2. The drain surfaces have been estimated around 0.2×0.2 μm for the NMOS and PMOS transistors. The supply voltage is 3.3 V.

Shallow Trench Isolation (STI) is used for isolation between the devices. The substrate process does not use an epitaxial layer. Fig. 3 depicts top views of the cell after polysilicon and metal 1 layer processing. Transistors N1 and P3 and the transistors N2 and P4 compose the inverter 1 and inverter 2, respectively. The transistors N5 and N6 are used as access transistors.

Three layers of metal and polysilicon gate are needed to make the SRAM cell functional: poly gate layer for WordLine strapping, M1 for internal hook-ups, VSS and VDD strapping, M2 for BitLines. The metal layer 1 has been built in Tungsten, while metal layer 2 and 3 used a stack of TiW/Al/TiW. These materials are known to impact the sensitivity of SRAM memory against the SEE risk [12], [14], [15]. Passivation and metal layers represent around 3.5 μm thick. A cross-section of the interconnects used on the process of the PMOS transistors is shown in Fig. 4. The detailed constitution of the interconnects of the SRAM memory has been deduced from the cross-section and are summarized in Table II.

The STI dimensions are revealed, with around 270 nm thick and 280 nm wide. The description of the interconnect process

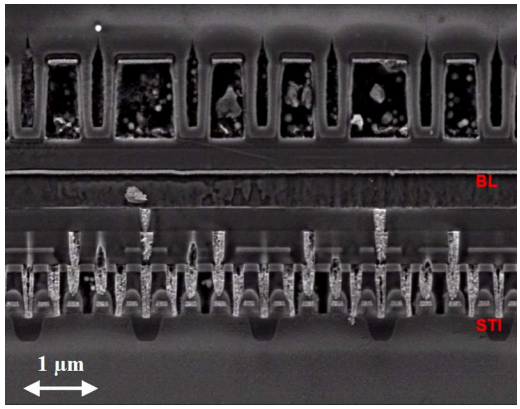

Fig. 4. Process cross-section showing passivation and metal layers obtained by reverse engineering of the Cypress 6T-SRAM memory.

TABLE II
SUMMARY OF MATERIALS USED FOR INTERCONNECT LAYERS AND THEIR CORRESPONDING THICKNESS

Layers	Materials	Thickness (nm)
Passivation	SiN / SiO	760 / 70
M3	TiW / Al / TiW	35 / 770 / 20
ILD2	SiO	315
M2	TiW / Al / TiW	30 / 335 / 30
ILD1	SiO	225
M1	W	325
ILD0	SIN / SiO / SiN / SiO	35 / 125 / 65 / 180
Cap	SiN	120
Siliciure	SiW	45
Poly	Poly Si	60

will be useful to define the device shielding in the platform MUSCA SEP^3/ADDICT.

The technological parameters of the studied memory are in agreement with the ITRS trends [13]. Reverse engineering and the technological trends [8] provided the junction acceptances of around 9×10^{-8} F.cm^{-1} and 8.5×10^{-8} F.cm^{-1} for N and PMOSFET respectively.

The presented device description leads to define the device model used in MUSCA SEP^3/ADDICT. As presented in the following section the sensitivity model used by the predictive platform will be adjusted and validated by grounds testing.

B. Radiation Ground Testing Results and SEU Estimations

This preliminary step aims at corroborating and validating the device description used in the electrical modeling (ADDICT) of the prediction platform. Several radiation ground testing have been done as presented previously. Cross-section measurements were made using a specific test vehicle (TIMES tester) embedding the SRAM memory (Fig. 5). The test fixture was developed by CNES.

The device was tested in dynamic mode with a checkerboard pattern at 3.3 V. In all campaigns, the test methodology consists in loading up the SRAM memory with a 5555 H (hexadecimal) word pattern and continuously scan it to detect errors

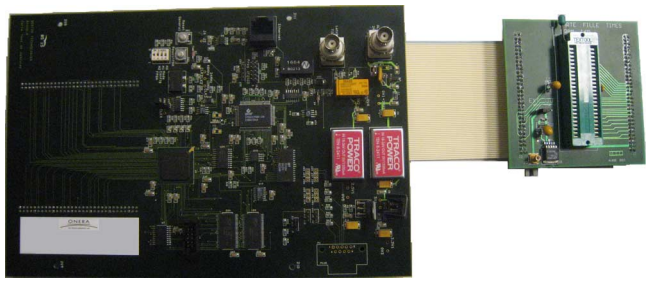

Fig. 5. Ground testing fixture (TIMES tester and daughterboard used for the ground testing campaign.

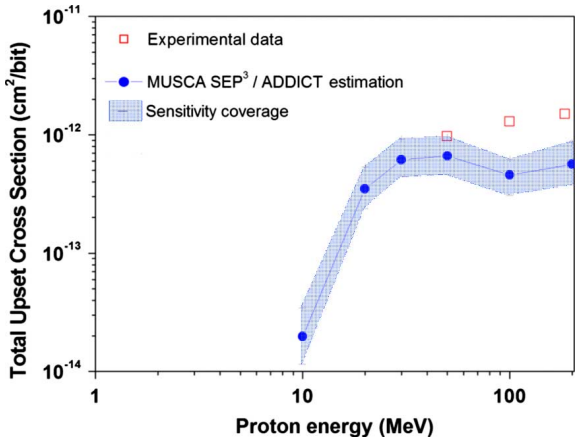

Fig. 6. Total upset cross-section measured for proton irradiation at KVI and calculated by MUSCA SEP^3/ADDICT prediction platform. The sensitivity coverages calculated with $\pm 25\%$ merging of the critical charge.

during the irradiation. Any detected erroneous word is immediately rewritten with the correct test pattern.

The main contributors to the global soft-error rate are clearly identified from simulations performed by MUSCA SEP^3/ADDICT: high-energy neutrons originating from cosmic rays in atmospheric environment; thermal neutron interactions with ^{10}B in the BoroPhosphor-Silicate Glass (BPSG) layer used during the manufacturing process. For Si technologies below the 0.18 μm technology node, BPSG is no longer used [16]. However, some sub-micro SRAM cells have been identified as having high thermal neutron SER [17]. Radiation ground testing on the chosen 90 nm SRAM memory were performed with thermal neutron beams at ILL. A very low cross section, $1 \times^{-16}$ cm^2/bit, was issued from these tests, thus providing evidences of the absence of BPSG layer in the studied device. This result leads to consider high-energy neutrons and protons as potential contributors to induce upsets on the SRAM memory.

A first comparison of the SEU cross-section was performed with the data collected during the ground testing at KVI. As depicted in Fig. 6, the high cross-section of the SRAM is around $\sim 9 \times 10^{-13}$ cm^2/bit and 1.4×10^{-12} cm^2/bit. Recent works provide data showing that the 90 nm Cypress memories have a cross-sections significantly higher (more than a decade) than other 90 nm SRAM memories [9]. The observed plateau trend is a known phenomenon for high energy protons [18]. The estimated SEU cross-section was calculated with MUSCA

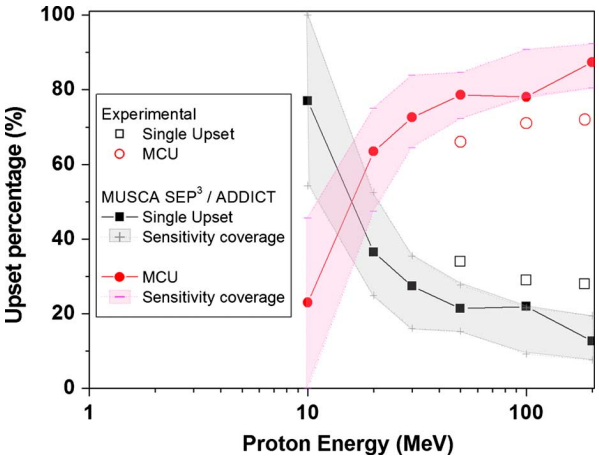

Fig. 7. Experimental data collected at KVI vs. calculations of the proportion between SEU and MCU for a range of proton energy. The sensitivity coverages calculated with $\pm 25\%$ merging of the critical charge.

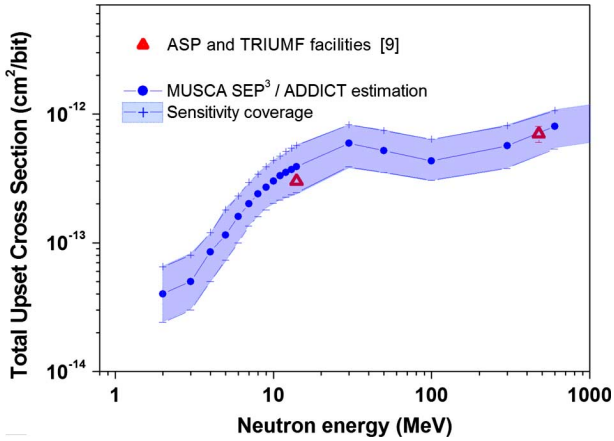

Fig. 8. The SEU cross-section calculated by the MUSCA SEP3/ADDICT platform (blue dots) for the SRAM memory under a neutron irradiation. Additional data (red triangles) are provided from 14 MeV neutron beam (ASP, AWE, Aldermaston, UK) and from 450 MeV neutron beam (TRIUMF, Vancouver, Canada) [9]. The sensitivity coverages calculated with $\pm 25\%$ merging of the critical charge.

SEP^3/ADDICT using as input the device model defined by the process description previously presented.

Fig. 6 demonstrates a relevant predictive SEU/MCU cross-section with the defined device model. Devices with 90 nm feature size are known to be susceptible to upset with a low critical charge under 1 fC. In the present device model, the mean critical charge has been adjusted at 0.1 fC and the FanOut1 parameter has been edited to 100 ps. The lower critical charge value emphasizes the strong sensitivity of the DUT [18]. The estimation coverage is calculated from a variation $\pm 25\%$ bracketing the mean value of the critical charge. The critical charge variation induces a coverage in fairly good agreement with the experimental data. A better modeling of the circuitry response of the memory should improve the cross-section estimation.

Fig. 7 presents in details the MCU contribution to the total SEU cross-section for a range of proton's energy between 10 MeV and 200 MeV. Experimental data reveal a light decreasing of the MCU percentage from 72% at 185 MeV to 66% at 50 MeV. The percentages of estimated upsets demonstrate the same global trend.

The last validation has been performed in order to compare the SEU estimation for a neutron beam. As shown in Fig. 8, the SEU cross-section calculated by MUSCA SEP^3/ADDICT has been compared with experimental data issued from literature [9] for a similar SRAM memory (part number CY62148EV30LL-45ZSXI). As previously, the sensitivity coverage is proposed for a critical charge variation ($\pm 25\%$ of the mean critical charge). Fig. 8 shows a fairly good agreement between results issued from experiments done at ASP and TRIUMF facilities [9] at 14 MeV and 450 MeV respectively and the estimated cross-section.

This validation of the device and the sensitivity model by ground tests represents a step forward for the operational prediction of the SRAM memory. Actually, the device has been included in the real life experimental platform in atmospheric environment. The comparisons between prediction and in-flight data are presented in the following section.

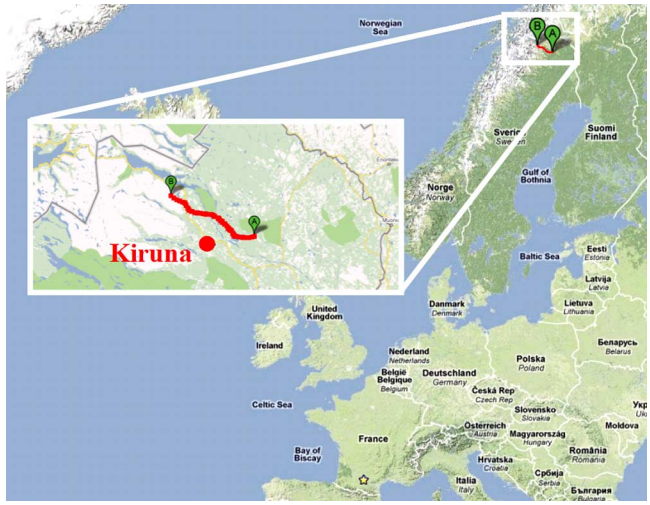

Fig. 9. Map of the course of the balloon flight, launched close to Kiruna (Sweden) in 2010.

IV. Operational Prediction

A. In-Flight Balloon Data vs. Prediction

A SRAM experimental platform including 1 Gbit (256 Mbit of the studied 90 nm SRAM) has flown as a piggy-back experiment during a balloon flight launched by CNES in 2010 in Kiruna, north of Sweden (67° latitude and 20° longitude). The experimental platform, so-called BALLTRAP, has been developed by TIMA to realize real-life SEU measurements on SRAMs operating in the atmospheric environment. Details about the testing board can be find in [6]. Five balloon flights have been performed for a total flight duration of about 45 hours. SEE events have been detected only during one flight. The flight lasts about 6 hours at an average altitude of $25 \sim 30$ km and with a maximum altitude around 43 km.

Fig. 9 depicts the course of the balloon flight launched in 2010 in Sweden. The balloon travelled around 100 km to the north

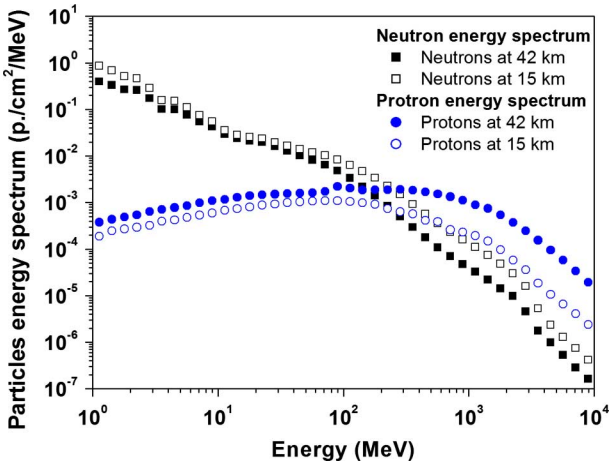

Fig. 10. Neutron and proton energy spectra modeled by QARM [20] for 42 km and 15 km, two representative altitudes of the profile of the balloon flight launched by the CNES in 2010 in Kiruna, north of Sweden (Lat. 67°, Long. 20°).

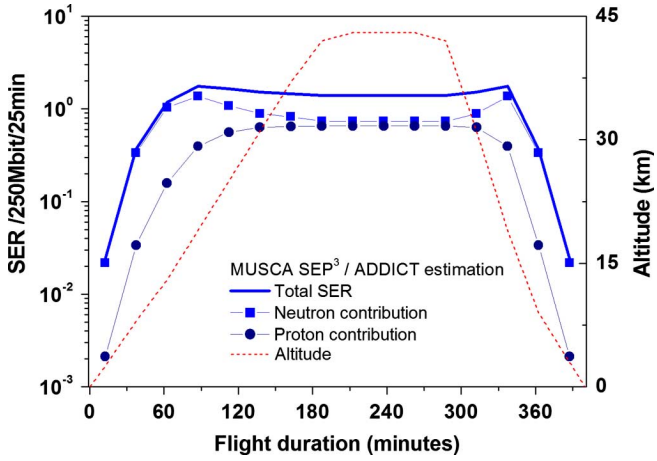

Fig. 11. Soft-Error Rate (SER) predicted for the BALLTRAP technological experiment on-board the stratospheric balloon. The neutron (blue squares) and proton (blue dots) contribution to the total SER (full blue line) is presented during the 6 hours of flight. The altitude of the balloon (red dash line) is also depicted.

west. The location data was provided by a GPS on-board the experiment.

The prediction platform performs the simulation with the relevant device model validated on ground testing as presented in the previous section. The radiation environment is modeled by a mixed isotropic flux of neutrons and protons. The differential flux of particles involved during the balloon flight has been simulated with the Qinetiq Atmospheric Radiation Model (QARM) [20]. Fig. 10 depicts the neutron and proton energy spectra for two representative altitudes of the profile of the balloon flight launched in 2010 in Kiruna.

Data collected by the experimental platform activated during the balloon flight, showed many upsets with a majority of MCU. The calculation performed by the prediction platform has been realized with the relevant mean model (device and sensitivity) validated in the previous section. The estimated SER for the experimental platform during the 6 hours of the 2010 balloon flight is depicted in Fig. 11. Over 30 km of altitude, neutrons and protons have a similar contribution to soft errors. The contribution of single and multiple errors to the total soft errors measured by the experimental platform is summarized in Fig. 12.

The number of observed errors, 13 soft errors (red bars), is correctly covered by the predictive calculations. The mean 90 nm device model validated in the previous section (median blue bars) announces 18 soft errors.

The contribution of single and multiple upsets to the total soft error number is pretty good estimated, as revealed in Fig. 12. The low and high sensitivity models correspond to a variation of $\pm 25\%$ of the critical charge (0.1 fC) of the 90 nm device model presented in the previous session. The prediction coverage overlaps fairly well in-flight data (red bars) of the SEU and MCU contribution.

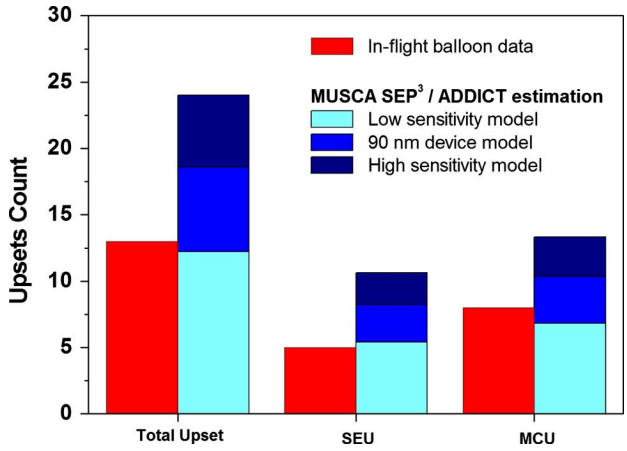

Fig. 12. Operational occurrence and rate of single and multiple upsets for the stratospheric balloon flight. The prediction coverage is depicted by low sensitivity model (lightly blue) and the high sensivity model (dark blue). The low and high sensitivity models correspond to a margin of $\pm 25\%$ of the critical charge of the 90 nm device model.

B. In-Flight Plane Data vs. Predictions

The last comparison of operational predictions has been performed for a commercial long-haul flight between Los Angeles and Paris. Results obtained during this flight are presented in detail in reference [6] for the same SRAM memory from Cypress. The integrated number of soft errors for the 6,5 hours duration of the flight (red triangles) is plotted in Fig. 13. As previously, the radiation environment is modeled by QARM, as illustrated in past works [6]. The number of observed errors, 15 soft errors (red triangle) is correctly covered by the prediction coverage (blue area). Besides, in comparison with previous estimations [6] (dark yellow bar), the presented methodology using MUSCA SEP^3/ADDICT leads to propose a better operational prediction, in terms of SEU number and coverage. The improvement of the operational prediction is mainly due to the relevant description of the device model and the validation of the sensitivity model by ground testing with neutron and proton beams.

C. Prospective Investigation of the Impact of Proton's Direct Ionization

Since a couple years, several works [5], [11], [21], [22] put in evidence the contribution of direct ionization of protons on

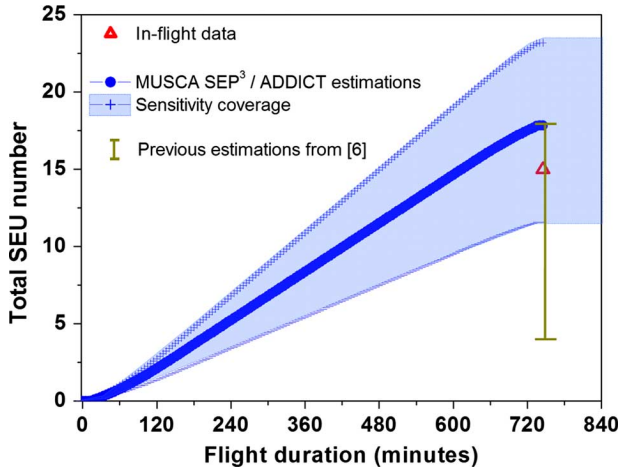

Fig. 13. Integrated SEU number calculated by MUSCA SEP^3/ADDICT with the mean sensitivity model for the 90 nm SRAM on-board a commercial long-haul flight from Los Angeles to Paris (blue colors). The real life platform has measured SEU events (red triangle) [6]. The dark yellow bar corresponds to the previous estimation.

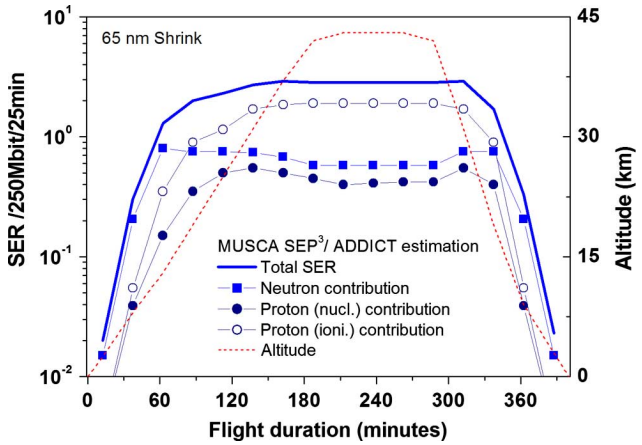

Fig. 14. Soft-error rate with the main contributors, the neutrons (blue squares), the nuclear protons (dark blue dots), the ionizing protons (empty blue dots) for a 65 nm technology virtually boarded in the 2010 balloon flight.

SER in space environment. This section aims at providing data showing-the significant impact on the SER of direct ionization of protons, this for a 65 nm SRAM memory operating in the Earth's atmosphere.

The investigation is based on the operational prediction of a 65 nm SRAM memory if the device has been boarded on the same stratospheric balloon flight previously presented. The 65 nm device model is defined using a shrink of the 90 nm SRAM memory with a high sensitivity model and a relevant technological description, i.e., with a depletion capacitance of around $150\,\mathrm{nF}/\mu\mathrm{m}$ and $125\,\mathrm{nF}/\mu\mathrm{m}$ for N and PMOSFET respectively [8], [13], [23]. The predicted in-flight SER with the main contributors versus flight duration is depicted in Fig. 14. The contribution of direct ionizing protons (empty blue dots) is clearly observed and over 30 km of altitude this mechanism is the main contributor.

These results emphasize the interest using stratospheric balloons to characterize in-flight integrated devices.

In future work, the real-life experiment platform will be redeveloped for more integrated SRAM memories, such as a 65 nm technology node. These experiments should corroborate the impact on the SEE sensitivity of 65 nm CMOS devices to atmospheric protons by direct ionization.

V. Conclusion

The sensitivity to natural radiation of a 90 nm commercial SRAM memory operating in the atmospheric environment was evaluated in details. The reverse engineering leads to define the device model used in the predictive platform. The device was tested with thermal neutrons and protons beams. The resulting experimental data were used to validate the device model and the SEU sensitivity model representative of the memory. The MUSCA SEP^3/ADDICT has been used to evaluate the SEE ground response and operational risk in the atmospheric environment. A good correlation with ground and in-flight SEU/MCU measures is exhibited. This work emphasizes the interest of stratospheric balloon flights in order to characterize and evaluate the operational risk of nanometric technologies.

The SRAM memory tested in this work was also selected to be included in the CARMEN -3, CNES experiment planned to fly on board the JASON3 satellite (orbit 1336 km, 63°) in 2013.

Acknowledgment

The authors would like to thank M. Lacourty and P. Chadoutaud, CNES, for their technical support during the balloon flight; F. Mialhe and G. Perez, CNES and C. De Nardi, Thales Group at CNES, for the reverse engineering of the investigated SRAM memory.

References

[1] H. May, "A new enemy-homotrons," *Int. Feder. Airline Pilots Assoc. (IFALPA) Newsletters*, 1980.
[2] A. Taber *et al.*, "Single-event effects in avionics," *IEEE Trans. Nucl. Sci.*, vol. 40, no. 2, pp. 120–126, Apr. 1993.
[3] E. Normand, "Single-event effects in avionics," *IEEE Trans. Nucl. Sci.*, vol. 43, no. 2, pp. 461–474, Apr. 1996.
[4] G. Hubert, S. Duzellier, F. Bezerra, and R. Ecoffet, "Operational SER calculations on the SAC-C orbit using the multi-scales single event phenomena predictive platform (MUSCA Sep3)," *IEEE Trans. Nucl. Sci.*, vol. 56, no. 6, pp. 3032–3042, Dec. 2009.
[5] G. Hubert, S. Bourdarie, L. Artola, S. Duzellier, C. Boatella-Polo, F. Bezerra, and R. Ecoffet, "Impact of the solar flares on the SER dynamics on micro and nanometric technologies," *IEEE Trans. Nucl. Sci.*, vol. 57, no. 6, pp. 3127–3134, Dec. 2010.
[6] P. Peronnard, R. Velazco, and G. Hubert, "Real-life SEU experiments on 90 nm SRAMS in atmospheric environment: measures versus predictions done by means of MUSCA SEP^3 platform," *IEEE Trans. Nucl. Sci.*, vol. 56, no. 6, pp. 3450–3455, Dec. 2009.
[7] L. Artola, G. Hubert, S. Duzellier, and F. Bezerra, "Collected charge analysis for a new transient model by TCAD simulations in 90 nm technology," *IEEE Trans. Nucl. Sci.*, vol. 57, no. 4, pp. 1869–1875, Aug. 2010.
[8] L. Artola, G. Hubert, K. M. Warren, M. Gaillardin, R. D. Schrimpf, R. A. Reed, R. A. Weller, J. R. Ahlbin, P. Paillet, M. Raine, S. Girard, S. Duzellier, L. W. Massengill, and F. Bezerra, "SEU prediction from SET modeling using multi-node collection in bulk transistors and SRAMs down to the 65 nm technology node," *IEEE Trans. Nucl. Sci.*, vol. 58, no. 3, Jun. 2011.
[9] A. Hands, P. Morris, C. Dyer, K. Ryden, and P. Truscoot, "Single event effects in power MOSFETs and SRAMs due to 3 MeV, 14 MeV and fission neutrons," *IEEE Trans. Nucl. Sci.*, 2011.

[10] R. A. Weller, R. A. Warren, R. A. Reed, K. M. Warren, M. H. Mendenhall, B. D. Sierawski, R. D. Schrimpf, and L. W. Massengill, "General framework for single event effects rate prediction in microelectronics," *IEEE Trans. Nucl. Sci.*, vol. 56, no. 6, pp. 3098–3108, Dec. 2009.

[11] B. D. Sierawki, J. A. Pellish, R. A. Reed, R. D. Schrimpf, K. M. Warren, R. A. Weller, M. H. Mendenhall, J. D. Black, A. D. Tipton, M. A. Xapsos, R. C. Baumann, X. Deng, M. J. Campola, M. R. Friendlich, H. S. Kim, A. M. Phan, and C. M. Seidleck, "Impact of low-energy proton induced upset on test methods and rate predictions," *IEEE Trans. Nucl. Sci.*, vol. 46, no. 6, pp. 3085–3092, Dec. 2009.

[12] H. H. K. Tang and E. H. Cannon, "SEMM-2: a modeling system for single event upset analysis," *IEEE Trans. Nucl. Sci.*, vol. 51, no. 3, Dec. 2004.

[13] ITRS, International Technology Roadmap for Semiconductor 2007.

[14] K. M. Warren, R. A. Weller, M. H. Mendenhall, R. A. Reed, D. R. Ball, C. L. Howe, B. D. Olson, M. L. Alles, L. W. Massengil, R. D. Schrimpf, N. F. Haddad, S. E. Doyle, D. McMorrow, J. S. Melinger, and W. T. Lotshaw, "The contribution of nuclear reactions to heavy ion single event upset cross-section measurements in a high-density SEU hardened SRAM," *IEEE Trans. Nucl. Sci.*, vol. 52, no. 6, Dec. 2005.

[15] R. A. Reed, R. A. Weller, M. H. Mendenhall, J.-M. Lauenstein, K. M. Warren, J. A. Pellish, R. D. Shcirmpf, B. D. Sierawski, L. W. Massengill, P. E. Dodd, M. R. Shaneyfelt, J. A. Felix, J. R. Schrawank, N. F. Haddad, R. K. Lawrence, J. H. Bowman, and R. Conde, "Impact of ion energy and species on single event effects analsysis," *IEEE Trans. Nucl. Sci.*, vol. 54, no. 6, Dec. 2007.

[16] R. C. Baumann and E. B. Smith, "Neutron-induced boron fission as a major source of soft errors in deep submicron SRAM devices," in *Proc. IRPS 2009*, pp. 152–157.

[17] S. Wen, R. Wong, M. Romain, and N. Tam, "Thermal neutron SPFT error rate for SRAM in the 90–45 nm technologie range," presented at the IEEE IRPS Symp., 2010.

[18] R. K. Lawrence and A. T. Kelly, "Single event effect induced multiple-cell upsets in a commercial 90 nm CMOS digital technology," *IEEE Trans. Nucl. Sci.*, vol. 55, no. 6, Dec. 2008.

[19] E. L. Petersen, J. C. Pickel, J. H. Adams, Jr, and E. C. Smith, "Rate prediction for single-event effects—a critique," *IEEE Trans. Nucl. Sci.*, vol. NS-39, pp. 1577–1577, 1992.

[20] Qinetiq Atmospheric Radiation Model [Online]. Available: http://geoshaft.space.qinetic.com/qarm

[21] D. Heidel, P. W. Marshall, K. A. Label, J. R. Schwank, K. P. Rodbell, M. C. Hakey, M. D. Berg, P. E. Dodd, M. R. Friendlich, A. D. Phan, C. M. Seidleck, M. R. Shaneyfelt, and M. A. Xapsos, "Low energy proton single-event upset test results on 65 nm SOI SRAM," *IEEE Trans. Nucl. Sci,.*, vol. 55, no. 6, pp. 3394–3400, Dec. 2008.

[22] J. A. Pellish, M. A. Xapsos, C. A. Stauffer, T. M. Jordan, A. B. Sanders, R. L. Ladbury, T. R. Oldham, P. W. Marshall, D. F. heidel, and K. P. Rodbell, "Impact of spacecraft shielding on direct ionization soft error rates for sub-130 nm technologies," *IEEE Trans. Nucl. Sci.*, vol. 57, no. 6, pp. 3183–3189, Dec. 2010.

[23] Z. Luo, A. Steegen, M. Eller, R. Mann, C. Baiocco, P. Nguyen, L. Kim, M. Hoinkis, V. Ku, V. Klee, F. Jamin, P. Wrschka, P. Shafer, W. Lin, S. Fang, A. Ajmera, W. Tan, D. Park, R. Mo, J. Lian, D. Vietzke, C. Coppock, A. Vayshenker, T. Hook, V. Chan, K. Kim, A. Cowley, S. Kim, E. Kaltalioglu, J. Ku, T. Schiml, J. Sudijono, I. Yang, and C. Wann, "High performance and low power transistors integrated in 65 nm bulk CMOS technology," presented at the Int. Electron Device Meeting, San Fransisco, CA, Dec. 2004.